A First Step to a Joint Stellarator Database

U. Stroth, G. Kühner, H. Maaßberg
Max-Planck-Institut für Plasmaphysik, EURATOM-IPP Association
D-85748 Garching, F.R.G.
M. Murakami, R.A. Dory
Oak Ridge National Laboratory, Oak Ridge, Tennessee, U.S.A.

IPP III / 195

Februar 1994

MAX-PLANCK-INSTITUT FÜR PLASMAPHYSIK

85748 GARCHING BEI MÜNCHEN

MAX-PLANCK-INSTITUT FÜR PLASMAPHYSIK

GARCHING BEI MÜNCHEN

A First Step to a Joint Stellarator Database

U. Stroth, G. Kühner, H. Maaßberg

Max-Planck-Institut für Plasmaphysik, EURATOM-IPP Association

D-85748 Garching, F.R.G.

M. Murakami, R.A. Dory

Oak Ridge National Laboratory, Oak Ridge, Tennessee, U.S.A.

IPP III / 195

Februar 1994

Die nachstehende Arbeit wurde im Rahmen des Vertrages zwischen dem Max-Planck-Institut für Plasmaphysik und der Europäischen Atomgemeinschaft über die Zusammenarbeit auf dem Gebiete der Plasmaphysik durchgeführt.

A First Step to a Joint Stellarator Database

U. Stroth, G. Kühner, H. Maaßberg

Max-Planck-Institut für Plasmaphysik, EURATOM-IPP Association,

D-85748 Garching, F.R.G.

M. Murakami, R. A. Dory

Oak Ridge National Laboratory, Oak Ridge, Tennessee, U.S.A.

Abstract

We report on a first step to an international stellarator database on global confinement data. The structure of the database is presented and a list of plasma parameters coveredis added as an appendix. The principal problems encountered in stellarator databases are discussed on the basis of ATF and W7-AS data. A simple comparison with tokamak data is made in terms of LHD and tokamak L-mode scaling expressions. Furthermore, some useful relations are derived to convert scaling expressions from machine to physics variables. Constraints deduced from these relations are used to compare regression expressions which follow Bohm-like or gyro-Bohm-like scalings. Finally, it is demonstrated that in the frame of linear regression analysis it is technically not possible to deduce a reliable dependence of the energy confinement time on the plasma energy.

1 Introduction

ATF and W7-AS have started to assemble a joint stellarator database for global confinement data. A modus operandi has been found and a detailed list of parameters for the data to be stored has been defined (see Appendix). It contains a minimum number of parameters which describe the device, discharge and plasma condition with sufficient accuracy. The datasets from each individual stellarator should represent the scaling properties found for the device. Data from other stellarators (CHS, Heliotron-E and W7-A) will be included in the near future. The database is still subject to modification, and suggestions from new contributors will be taken into account.

The objectives of the database are:

availability of comparable global confinement databases for different stellarators;

creation of a basis for investigating the influence of the magnetic field configuration on confinement;

determination of a reliable scaling law for stellarator properties to predict the performances of future stellarator devices.

The joint database might be combined with a comparable tokamak database. The parameters are chosen and named by analogy with the existing ITER databases to facilitate possible linking of the databases.

2 Overview of the database

At presentl, 438 ATF and W7-AS discharges are stored in the database. The composition of the database is listed in Tab. 1, discharges done in He being ignored. It can be seen that the line-averaged density $\bar{n}_e$, magnetic field strength B, and absorbed heating power P are sufficiently varied to perform regression analyses. There are, however, more neutral-beam-heated discharges (NBI) in ATF and more ECRH discharges in W7-AS. NBI heating is correlated with high density, and hence most of the high-density discharges are from ATF.

There are no variations in the edge rotational transform ι_a and minor plasma radius a in ATF and almost no variation in the isotope mass m in the W7-AS data. The isotope scaling can therefore only be studied in ATF, and a and ι_a scalings only in W7-AS. The major radius is about the same in the two devices ($R \simeq 2\ m$). This reduces the number of free parameters when comparing the two devices.

3 Lack of information

In principle, the possibly different levels of confinement in ATF and W7-AS could come from the different minor radii, the higher ι_a of ATF or the differences in the magnetic configuration (ATF has strong magnetic shear, W7-AS a very weak one). If the ι_a and a dependences found for W7-AS alone are applied to ATF, any difference in confinement might be attributed to the different magnetic configurations. The main problem, however,

Device	Heating	N	P	$\bar{n}_e$	B	ι_a	ι_0	a	m
ATF	Combined	53	0.2-1.13	0.43-4.74	0.45-1.89	1	0.22-0.41	0.27	1-2
	ECRH only	53	0.05-0.41	0.33-1.04	0.64-1.89	1	0.22-0.33	0.27	1-2
	NBI only	127	0.27-1.48	1.31-11	0.45-1.91	1	0.15-0.46	0.27	1-2
W7-AS	Combined	5	0.42-1.11	2.25-6	2.53-2.56	0.35-0.5	0.35-0.5	0.16-0.18	1.5-2
	ECRH only	144	0.51-2	0.42-8.4	1.31-2.57	0.31-0.59	0.31-0.59	0.12-0.19	1-2
	NBI only	52	0.35-3	3.17-23.3	1.1-2.59	0.32-0.63	0.32-0.63	0.12-0.18	1.5-2

Table 1: Number of observations and ranges (minimum-maximum) of the plasma parameters stored in the database for the various devices and heating scheems.

is how the scaling with the edge ι value, which can be well studied in one device alone, can be applied to inter-device scalings where the devices have distinctly different ι profiles.

Including CHS, Heliotron-E and W7-A data will help to determine the size scaling from device to device. For example, CHS has a smaller R (0.95 m) and roughly the same a (0.19 m) as W7-AS and Heliotron-E has the same geometrical dimensions as W7-AS but a magnetic configuration similar to ATF.

4 The global energy confinement

For the regression studies we use the following physical units: Confinement time τ_E in ms, line-averaged density in 10^{19} m^{-3}, magnetic field strength in T, heating power in MW, minor and major radii in m and isotope mass m in atomic units. The diamagnetic energy measurement is used for the energy confinement time.

4.1 Scaling of the individual devices

We start with a regression for the entire ATF dataset. Among the data there are only 53 pure ECRH discharges. A scaling of the entire dataset yields

$$\tau_E^{ATF_a} = 4.12 \times P^{-0.58\pm0.04}\bar{n}_e^{0.50\pm0.02}B^{0.77\pm0.05}m^{-0.02\pm0.05} \quad 233 \text{ obs., rmse} = 0.238. \tag{1}$$

Hence, there is no isotope effect in ATF. The corresponding scaling expression for the W7-AS dataset is

$$\tau_E^{W7AS_a} = 64.76 \times P^{-0.56\pm0.03}\bar{n}_e^{0.53\pm0.03}B^{0.72\pm0.06}\iota_a^{0.29\pm0.08}a^{1.84\pm0.12} \quad 199 \text{ obs., rmse} = 0.219. \tag{2}$$

For this scaling m had to be omitted but the data can give information about the a and ι_a scalings. The dependences on $\bar{n}_e$, B and P are very similar to those in ATF. Distinct differences, however, are noticed if the dataset is restricted to ECRH discharges only. A standard dataset of discharges without NBI heating yields the following result:

$$\tau_E^{W7AS_{ECH}} = 79.6 \times P^{-0.53\pm0.04} \bar{n}_e^{0.70\pm0.05} B^{0.61\pm0.07} \iota_a^{0.31\pm0.1} a^{1.92\pm0.14}$$
$$136 \text{ obs., rmse} = 0.204. \tag{3}$$

The confinement of these discharges, which are restricted to low densities (ECRH cut-off), scales more strongly with the density and more weakely with the magnetic field. The dependence on the heating power turns out to be very resilient to changes in the dataset selection. The question whether the stronger density scaling with ECRH only is related to the lower density or to the different heating method is difficult to answer since, for the time being, almost all high-density discharges are with NBI. In the near future, however, high-density data with pure ECRH at 140 GHz will be included from W7-AS.

Unfortunately, the 53 ECRH-only discharges from ATF do not allow a full regression analysis. The fit yields a very uncertain B scaling and also a much stronger density dependence:

$$\tau_E^{ATF_{ECH}} = 4.78 \times P^{-0.52\pm0.07} \bar{n}_e^{0.78\pm0.11} B^{0.20\pm0.17} m^{0.05\pm0.09}$$
$$53 \text{ obs., rmse} = 0.213. \tag{4}$$

4.2 Scaling of the joint dataset

In order to get a scaling expression for the joint database, the following assumption is made: Since the a scaling can be determined from W7-AS, we impose the dependence on a as found in Eq. 2. Then we regress the joint database, using either an unconstrained ι_a dependence

$$\tau_E^{j_a} = 43.9 \times P^{-0.57\pm0.03} \bar{n}_e^{0.50\pm0.02} B^{0.78\pm0.04} \iota_a^{-0.05\pm0.03} a^{1.84} m^{0.03\pm0.04}$$
$$432 \text{ obs., rmse} = 0.232, \tag{5}$$

or we impose the dependence as found for W7-AS alone (Eq. 2),

$$\tau_E^{j_b} = 43.4 \times P^{-0.62\pm0.03} \bar{n}_e^{0.51\pm0.02} B^{1.01\pm0.03} \iota_a^{0.29} a^{1.84} m^{0.15\pm0.05}$$
$$432 \text{ obs., rmse} = 0.259. \tag{6}$$

The two results are plotted in Fig. 1. Imposing the ι_a dependence handicaps the ATF confinement and the regression gets worse (see the rmse). Two interpretations are possible: (i) The confinement depends neither on ι_a nor the magnetic configuration, or (ii) the ι_a scaling as found from W7-AS, which goes in the same direction as for tokamaks, is correct. It must then be concluded that ATF confinement is relatively inferior to W7-AS confinement and this could be due to the magnetic configuration (possibly to the magnetic shear). As mentioned above, it is doubtful, however, whether the ι scaling found from a low-shear device can be used when one compares with a strong shear device having a rather high edge ι value. The difference of the two scaling expressions becomes weaker if one uses for ATF the ι values at $r/a = 0.6$ instead of the edge value. This would lower the ι value of ATF from 1 to about 0.6 and make the difference to that of W7-AS small. This is similar to omitting ι as regressor. We come back to this point in section 5.

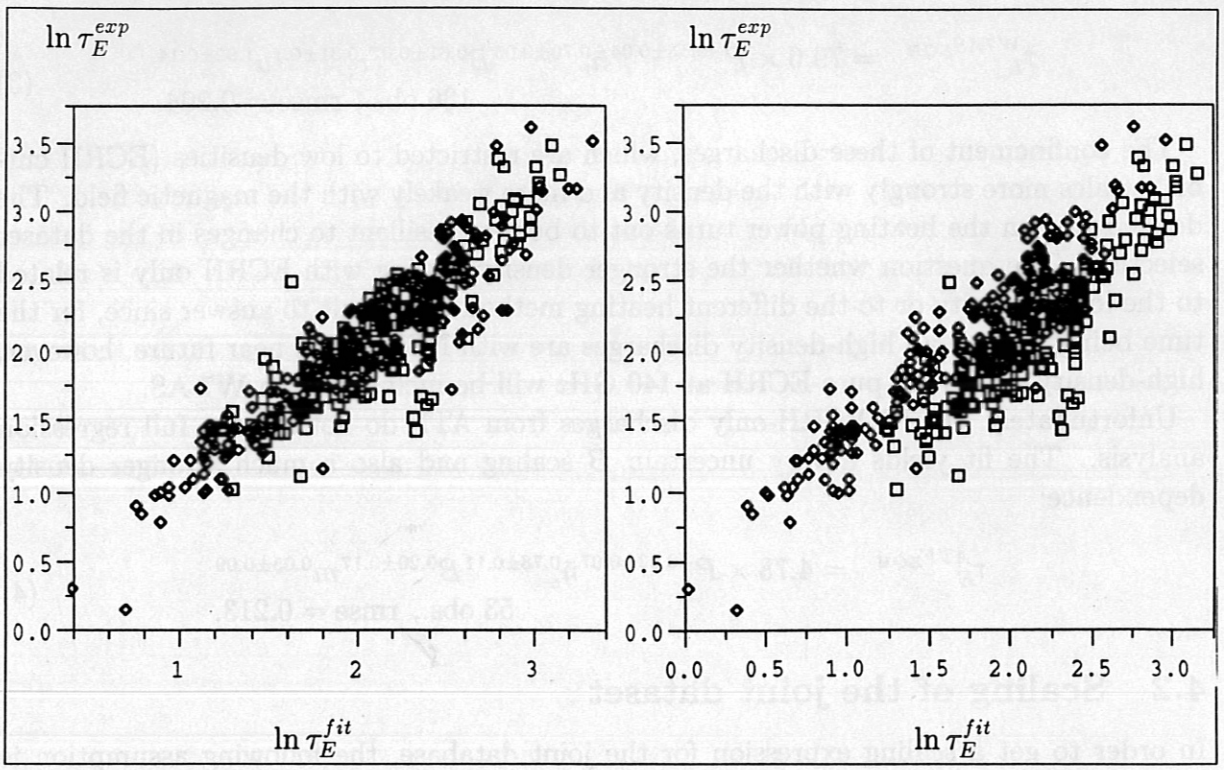

Figure 1: Regression of the joint ATF/W7-AS database (□ and ◇, respectively) leaving ι_a unconstrained (Eq. 5, left) or constraining it to 0.29 (Eq. 6, right).

4.3 Bohm- or gyro-Bohm-like scaling expressions

An important question for extrapolation to larger devices is whether the confinement follows a Bohm-like or gyro-Bohm-like scaling expression. This question cannot be answered from global databases alone. In order to demonstrate this, we compare an unconstrained fit of the joint database (similar to that of Eq. 5, but now with an unconstrained a dependence) with fits where Bohm- or gyro-Bohm-like constraints have been imposed (see Eq. 9 for the constraints).

The scaling expression for the Bohm constraint reads

$$\tau_E^{jB} = 0.89 \times P^{-0.62} n^{0.52} B^{0.68} \iota_a^{0.02} a^{1.58}, \tag{7}$$

and for the gyro-Bohm one

$$\tau_E^{jgB} = 0.89 \times P^{-0.53} n^{0.49} B^{0.87} \iota_a^{0.13} a^{1.57}. \tag{8}$$

The transformation of a scaling expression of the form $\tau \sim P^{\alpha_P} n^{\alpha_n} B^{\alpha_B} a^{\alpha_a}$ (to use this formula, R and the plasma current I have to be transformed into $q = 1/\iota_a$, a and aspect ratio) into the form $\tau/\tau^{Bohm} \sim \rho_*^{\alpha_\rho} \beta^{\alpha_\beta} \nu_*^{\alpha_\nu} a^{\alpha_a}$ is done with the help of

$$\alpha_a = \frac{\frac{1}{2}\alpha_P - 2\alpha_n - \frac{5}{4}\alpha_B + \alpha_a}{1+\alpha_P} - \frac{5}{4},$$

$$\alpha_\rho = \frac{-3\alpha_P - 2\alpha_n - \frac{6}{4}\alpha_B}{1+\alpha_P} + \frac{1}{2},$$

$$\alpha_\beta = \frac{\frac{3}{2}\alpha_P + \alpha_n + \frac{1}{4}\alpha_B}{1+\alpha_P} + \frac{1}{4},$$
$$\alpha_\nu = \frac{-\frac{1}{2}\alpha_P - \frac{1}{4}\alpha_B}{1+\alpha_P} - \frac{1}{4}. \quad (9)$$

A scaling expression can be called dimensionally correct if $\alpha_a = 0$; Bohm or gyro-Bohm constraints can be constructed out of $\alpha_\rho = 0$ or $\alpha_\rho = -1$, respectively. The above results then have the following forms:

Unconstrained fit:

$$\tau^{j_a}/\tau^{Bohm} \sim \rho_*^{-0.53}\beta^{-0.15}\nu_*^{-0.03}, \ \text{rmse} = 0.229, \quad (10)$$

Bohm-constrained fit (eq. 7):

$$\tau^{j_B}/\tau^{Bohm} \sim \rho_*^{0}\beta^{-0.36}\nu_*^{0.12}, \ \text{rmse} = 0.233, \quad (11)$$

gyro-Bohm constrained fit (Eq. 8):

$$\tau^{j_{gB}}/\tau^{Bohm} \sim \rho_*^{-1.0}\beta^{0.06}\nu_*^{-0.15}, \ \text{rmse} = 0.232. \quad (12)$$

Although the results are very different in their parameter dependences, the qualities of the different fits are very similar. This is a sign of collinearity in the dimensionless parameters. This collinearity is broken in dimensionally similar discharges [1, 2]. From global scalings no firm conclusion about the leading ρ_* dependence can be drawn. The unconstrained fit of the pure ECRH W7-AS dataset yields an almost pure gyro-Bohm ρ_* dependence.

4.4 The use of local quantities; correlated errors

In section 4.3 the analysis was done in terms of engineering variables. It would also be desirable to do this analysis direct in terms of the dimensionless physics variables. In particular, one would like to see the power P replaced by a local quantity such as the temperature T_e, calculated from, for example, the energy content W. This is dangerous, however, because W would then be use (in τ_E) as dependent and (as regressor) independent variables. This introduces correlated errors which are very difficult to treat. To demonstrate this, we have made up a database of 625 imaginary observations constructed in the following way:

$$\begin{aligned} P &= 1,2...5 \ , \\ B &= 1,2...5 \ , \\ n &= 1,2...5 \\ \Rightarrow \quad \tau_E &= P^{-0.6}n^{0.6}B^{0.8}, \\ W &= \tau_E \times P. \end{aligned} \quad (13)$$

For each combination of values for n, B and P five identical observations are stored and used in some cases to add statistical errors. With this dataset, two types of regressions were performed, one using the machine variables and the other using W instead of P as regressor. Both ways should, of course, give the same results. And this is indeed the case

if the set is used without statistical errors, as given by Eqs. 13. In the second case, the result is

$$\begin{aligned} \tau_E &= W^{-1.5} n^{1.5} B^2, \\ &\text{rmse} = 10^{-10}. \end{aligned} \tag{14}$$

Simple algebra shows that this is in agreement with the expression for τ_E in Eq. 13. A more realistic situation is achieved if a random error is introduced to the data. Random errors in n, B and P have only weak influence on the scaling results. The effect is strong, however, if one uses

$$\tau_E = P^{-0.6} n^{0.6} B^{0.8} \times (1 + 10\% \text{ random error}). \tag{15}$$

The two types now of regression give the following results:

$$\begin{aligned} \tau_E &= P^{-0.604 \pm 0.007} n^{0.611 \pm 0.007} B^{0.801 \pm 0.007}, \\ &\text{rmse} = 0.106, \end{aligned} \tag{16}$$

$$\begin{aligned} \tau_E &= W^{-1.07 \pm 0.04'} n^{1.27 \pm 0.03} B^{1.66 \pm 0.04} \\ &\text{rmse} = 0.241. \end{aligned} \tag{17}$$

The scaling using machine variables is still correct, whereas a misleading result is obtained as soon as P is replaced by W. A similar effect is introduced if a hidden variable is taken into account. For that purpose, we design our dataset as in Eq. 13 and add the variable h:

$$\begin{aligned} h &= 1, 2 \ldots 5 \\ \Rightarrow \quad \tau_E &= P^{-0.6} n^{0.6} B^{0.8} h^{0.2}, \\ W &= \tau_E \times P. \end{aligned} \tag{18}$$

Here, no statistical error is used. h is supposed to contribute to the confinement scaling, but it is omitted in the regressions. The results of the two types of regressions are

$$\begin{aligned} \tau_E &= P^{-0.6} n^{0.6} B^{0.8} \\ &\text{rmse} = 0.114, \end{aligned} \tag{19}$$

$$\begin{aligned} \tau_E &= W^{-1.00 \pm 0.04} n^{1.2 \pm 0.03} B^{1.6 \pm 0.04} \\ &\text{rmse} = 0.225. \end{aligned} \tag{20}$$

Again, the result with W is misleading. The correlated error was now only introduced by a hidden variable which in realistic data could be, for example, the machine conditions.

Linear regression analysis is not adequate to handle this type of correlation. Nonlinear schemes[1] could help to overcome this problem.

5 Comparison with tokamak L-mode confinement

One objective is to compare stellarator confinement with tokamak confinement. As reference for tokamak confinement we use the ITER L-mode database[2]. The comparison is

[1] e.g. as developed by V. Dose at IPP

[2] kindly provided by S. Kaye

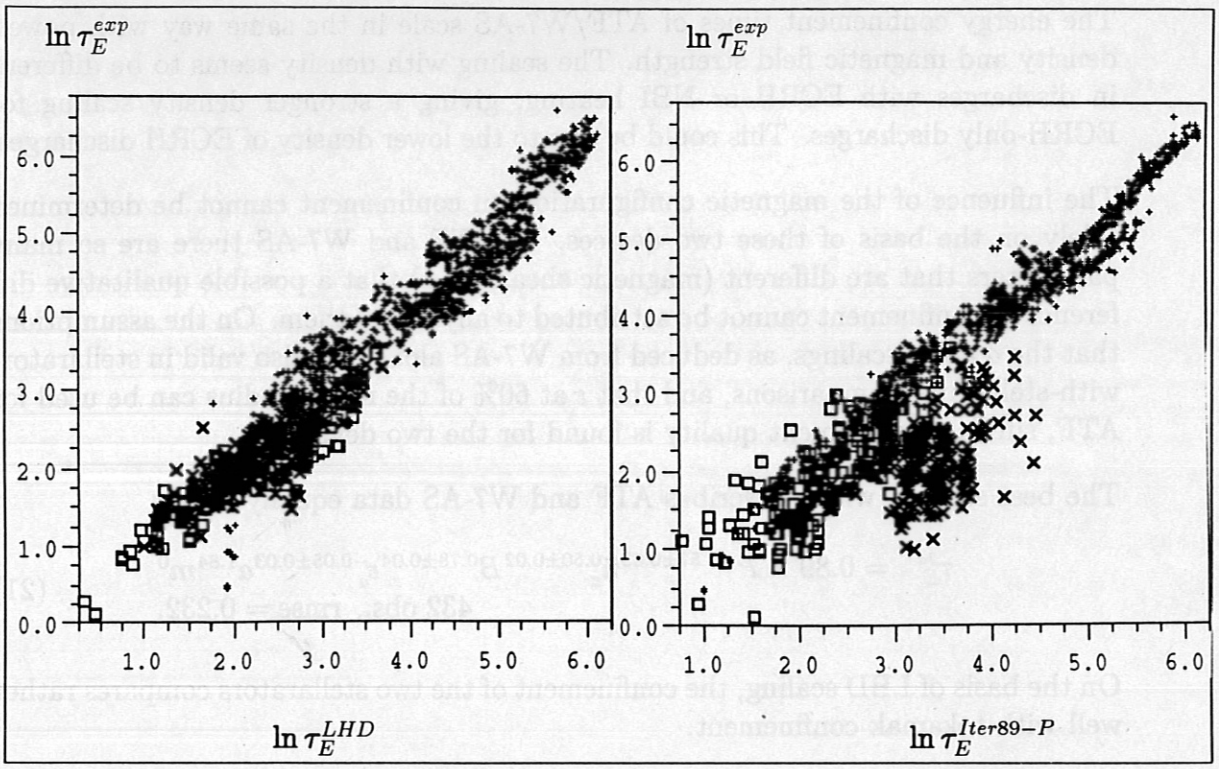

Figure 2: Comparing the joint database with the ITER L-mode database on the basis of LHD scaling ([3], left) and ITER89-P scaling ([4], right). ATF, W7-AS and tokamaks are represented by $\times$, $\square$ and $+$ signs, respectively

made on the basis of two different scaling laws: (i) the LHD [3] scaling, which can be directly applied to stellarators and (ii) ITER89-P [4], which is a tokamak L-mode scaling expression. For (i) the tokamak current was replaced by ι_a and B, and for (ii) we calculated for stellarators an equivalent current from ι_a. Absolute normalisation of both scaling expressions was done with respect to the tokamak data only.

The comparison of the ATF and W7-AS data with the tokamak L-mode database on the basis of the two scaling expressions is depicted in Fig. 2. The confinement of W7-AS and the tokamaks can be described rather well by both scaling laws. On the basis of LHD scaling, also ATF agrees very well with the other data. Since the ITER89-P scaling uses a very strong q or ι_a dependence (originating from the current scaling), ATF shows a somewhat lower confinement. Very probably, however, the edge ι value is not a good parameter when comparing devices of different ι profiles (the profile of the ATF torsatron has the inverse shape of a tokamak profile). Again, the difference becomes smaller (see 4.2) if an averaged ι instead of ι_a is used, because then the ι values of the different devices come closer together.

6 Summary

The results of a first analysis of a joint ATF/W7-AS global database are:

The energy confinement times of ATF/W7-AS scale in the same way with power, density and magnetic field strength. The scaling with density seems to be different in discharges with ECRH or NBI heating, giving a stronger density scaling for ECRH-only discharges. This could be due to the lower density of ECRH discharges.

The influence of the magnetic configuration on confinement cannot be determined solely on the basis of these two devices. In ATF and W7-AS there are so many parameters that are different (magnetic shear, ι_a, a) that a possible qualitative difference in confinement cannot be attributed to any one of them. On the assumptions that the a and τ scalings, as deduced from W7-AS alone, are also valid in stellarator-with-stellarator comparisons, and that τ at 60% of the minor radius can be used for ATF, similar confinement quality is found for the two devices.

The best scaling, which describes ATF and W7-AS data equally well is

$$\tau_E^{ja} = 0.89 \times P^{-0.57\pm0.03} \bar{n}_e^{0.50\pm0.02} B^{0.78\pm0.04} \iota_a^{-0.05\pm0.03} a^{1.84} m^0 \qquad (21)$$
$$432 \text{ obs., rmse} = 0.232.$$

On the basis of LHD scaling, the confinement of the two stellarators compares rather well with tokamak confinement.

This database is a first step to an international database. Firmer conclusions can be drawn when data from Heliotron-E, CHS and W7-A are included in the near future.

References

[1] WALTZ, R. E., DeBOO, J. C., and ROSENBLUTH, M. N., Phys. Rev. Lett. **65** (1990) 2390.

[2] STROTH, U., KÜHNER, G., MAASSBERG, H., and RINGLER, H., Phys. Rev. Lett. **70** (1993) 936.

[3] SUDO, S., TAKEIRI, Y., ZUSHI, H., SANO, F., ITOH, K., et al., Nucl. Fusion **30** (1990) 11.

[4] YUSHMANOV, P. N., TAKIZUKA, T., RIEDEL, K. S., KARDAUN, O. J. W. F., CORDEY, J. G., et al., Nucl. Fusion **30** (1990) 1999.

Appendix

Descriptions of parameters stored in the Stellarator Database

23.12.1993

General Comments

Missing data or data which are not available are characterized by -9999999 for integers, -9.999E-09 for real and *NODATA* for characters

Heating powers which are not applied are set to 0 and additional information (i.e. PGASA, FECH1, ...) for heating which is not applicable are set to be "missing" (see above).

1. General parameters

1. STELL — Stellarator that has supplied the data:
ATF, CHS, HEL-E, L2, W7-A, W7-AS; (in locus, 1=ATF; 2=W7-AS; 3=HEL-E; 4=CHS; 5=W7-A)

2. UPDATE — last update [YYMMDD]

3. DATE — Date that the shot was taken [YYMMDD]

4. SHOT — Shot number or the first shot number of a sequence

5. SEQ — Sequence number (designated for a series of similar shots)

6. TIME — Time during the shot at which the data are taken [s]

7. PHASE — Phase of the discharge:
STAT = stationary phase
DRAMP = density ramp
...

2. Plasma composition

8. PGASA — Mass number of plasma working gas:
1= H_2; 2= D_2; 3=He_3; 4=He_4

9. BGASA — Mass number for NBI gas:
1= H2; 2= D2; 3=He_3; 4=He_4

10. RGEO Plasma geometrical major radius [m]
ATF: (Rmax+Rmin)/2
W7-AS: 2 m + vertival shift

11. RMAG Major radius [m].of the magnetic. axis in the vacuum geometry
W7-AS: 2.05 m + vertival shift

12. AEFF Effective minor radius [m]
W7-AS: From simple formula interpolating between available configurations

13. SEPLIM Minimum distance between the separatrix and the wall or the limiter [m]
W7-AS: =0 if Min(RLIMTOP-RLIMBOT)-AEFF < 0.005 m

14. CONFIG Plasma configuration
STAN = standard
ATF: for future use
W7-AS: CDMOOF = current drive (CD), heat modulated (MO), off-axis ECH (OF)

3. Machine conditions

15. WALMAT Material of the vacuum vessel wall:
IN = inconel
INCARB = inconel with carbon
SS = stainless steel
SSCARB = stainless steel with carbon

16. LIMMAT Limiter material:
C = carbon
BORC = Boron-carbide
TIC = titanium coated graphite

17. EVAP Evaporated material:
C = carbonized
BOR = boronized
TI = titanium
NONE = no evaporation
ATF: 5 = BOR; 6 = C; 22 = TI; 0 = NONE

4. Magnetics

18. BT Vacuum toroidal field at RGEO [T]
ATF: calculated from coil current

19. IP — Total plasma current [A] positive if it increases the vacuum iota (equivalent to the direction of a tokamak current)

20. VSURF — Loop voltage at plasma boundary [V]: (+) giving positive IP

21. IOTAA — Iota_bar at plasma edge (AEFF)
W7-AS: From simple formula interpolating between available configurations

22. IOTA0 — Iota_bar at the plasma center
ATF: iota = iota0*(1-x^2)+iotaa*x^2; for a "global" iotabar,
iota = iotabar(rho=2/3) = 0.555*iota0+0.444*iotaa based on parabolic iotabar(rho) and rho=3/2
W7-AS: From simple formula interpolating between available configurations

23. BETDIA — Toroidal beta based on diamag. measurement (fraction, not %)

24. NEBAR — Central line average electron density in [m^{-3}] from a laser or microwave interferometer
W7-AS: If available, from microwave interferometer, otherwise from central HCN chord.

25. DNEBDT — Time-derivative of NEBAR in [m^{-3}/s]
ATF: only steady state -> set to 0
W7-AS: only steady state -> set to 0

5. Impurities

26. ZEFF — Average plasma effective charge
W7-AS: missing

27. PRAD — Total radiative power as measured with bolometry [W]
W7-AS: for shot > ? from upper camara (*)

6. Input power

28. PECH1 — Portthrough power for primary ECH [W]
W7-AS: sum of 70 GHz powers

29. PECH2 — Portthrough power for secondary ECH [W]
W7-AS: sum of 140 GHz powers

30. MECH1 Mode of primary ECH:
1 = fundamental; 2 = 2nd harmonic ....

31. MECH2 Mode of secondary ECH:
1 = fundamental; 2 = 2nd harmonic ....

32. PABSECH Total absorbed ECH power [W]
W7-AS: 90% and 100% absorption in first and 2nd harmic, respectively

33. ENBI1 Power-weighted neutral beam energy for the primary beams [V]
W7-AS: Sources 1+5; 1:1/2:1/3 = 1:1:1

34. ENBI2 Power-weighted neutral beam energy for the secondary beams [V]
W7-AS: Sources 3+7; 1:1/2:1/3 = 1:1:1

35. RTAN1 Tangency radius for the primary beams
W7-AS: 1.95 m

36. RTAN2 Tangency radius for the secondary beams
W7-AS: 1.85 m

37. PNBI1 Portthrough NBI power for the primary beams [W]
= 0 if no NBI was applied

38. PNBI2 Portthrough NBI power for the secondary beams [W]
= 0 if no NBI was applied

39. PABSNBI Total absorbed NBI power [W]
= 0 if no NBI was applied
ATF: absorbed power calculated with a formula
W7-AS: according to simple formula deduced from Fafner calculations

40. PICH Portthrough ICRF power [W]

41. FICH ICRF frequency [Hz]

42. PABSICH ICRF absorbed power [W]
= 0. if no ICH was applied

43. POH Ohmic heating power [W]

7. Temperatures

44. NE0 Central electron density at RMAG [m^{-3}]
W7-AS: taken from a fit to a Thomson scattering profile

45. TE0 Central electron temperature at RMAG [eV]
W7-AS: taken from a fit to a Thomson scattering profile

8. Energies

46. WDIA Total plasma stored energy as determined by diamagnetic measurements [J]

47. WMHD Total plasma stored energy as determined with MHD equilibrium [J]

48. WETH Total thermal electron plasma energy [J]
W7-AS: from Thomson scattering profiles

49. WITH Total thermal ion plasma energy [J]
W7-AS: from simulation with neoclassical transport coefficient,

50. WTH Total thermal plasma energy from kinetic meas.urements [J]

51. WFPER Total perpendicular fast ion energy calculated [J]
W7-AS: missing

52. WFPAR Total parallel fast ion energy calculated [J]
W7-AS: missing

9. Energy confinement times

53. TAUEDIA Global confinement time [s] based on diamagnetic measurrement
TAUEDIA = WDIA/(PABSECH+PABSNBI+PABSICH+POH-dWDIA/dt)
W7-AS: dWDIA/dt = 0 is used
ATF: dWDIA/dt = 0 is used

54. TAUETH Thermal energy confinement time [s]
TAUETH = WTH/(PABSECH+PABSNBI+PABSICH+POH-dWTH/dt)
W7-AS: dWTH/dt = dWDIA/dt) is used

10. Extra information

55. COFRANBI Ratio of co-injected beam power to total NBI power
W7-AS: If BT>0 => Sources(5+6+7+8)/all sources

56. STDSET Standard data set =1